Baryon number fluctuations
and singularities at real and complex baryochemical potential

Volodymyr Vovchenko

ITP & FIAS, Goethe University Frankfurt

V.V., A. Pásztor, Z. Fodor, S.D. Katz, H. Stoecker, Phys. Lett. B 775, 71 (2017)

V.V., J. Steinheimer, O. Philipsen, H. Stoecker, arXiv:1711.01261

V.V., L. Jiang, M.I. Gorenstein, H. Stoecker, arXiv:1711.07260

EMMI Workshop "Constraining the QCD Phase Boundary with Data from Heavy Ion Collisions"

GSI, Darmstadt, Germany

February 12, 2017

Outline

- Motivation: QCD equation of state at finite baryon density
- New lattice QCD data at imaginary μ_B
  - Fourier coefficients of fugacity expansion
  - Evidence for baryonic excluded volume
- Cluster expansion model
  - Baryon number susceptibilities
  - Radius of convergence and Roberge-Weiss transition
- Critical point of nuclear matter and beam energy dependence of net proton number fluctuations
- Summary

Analysis of new lattice data at imaginary chemical potential using the fugacity expansion

V. Vovchenko, A. Pásztor, Z. Fodor, S.D. Katz, H. Stoecker, Phys. Lett. B 775, 71 (2017)

QCD thermodynamics with fugacity expansion

QCD thermodynamics with relativistic fugacity/cluster expansion:

$$\frac{p(T,\mu_B)}{T^4} = \sum_{k=0}^{\infty} p_k(T) \cosh\left(\frac{k\,\mu_B}{T}\right) = \sum_{k=-\infty}^{\infty} \tilde{p}_{|k|}(T)\, e^{k\mu_B/T}$$

Imaginary μ_B: no sign problem on the lattice

$\mu_B \to \mathrm{i}\tilde{\mu}_B \quad \Rightarrow \quad$ observables obtain trigonometric Fourier series form

Pressure: $$\frac{p(T,\mathrm{i}\tilde{\mu}_B)}{T^4} = \sum_{k=0}^{\infty} p_k(T) \cos\left(\frac{k\,\tilde{\mu}_B}{T}\right),$$

Baryon density: $$\frac{\rho_B(T,\mathrm{i}\tilde{\mu}_B)}{T^3} = \mathrm{i}\sum_{k=1}^{\infty} b_k(T) \sin\left(\frac{k\,\tilde{\mu}_B}{T}\right), \quad b_k(T) \equiv k\, p_k(T)$$

$$b_k(T) = \frac{2}{\pi\, T^4} \int_0^{\pi T} d\tilde{\mu}_B\, [\mathrm{Im}\,\rho_B(T, i\tilde{\mu}_B)] \sin(k\,\tilde{\mu}_B/T)$$

Coefficients $b_k(T)$ can and are now being calculated in LQCD

We analyze $b_k(T)$ with phenomenological models directly at Im μ_B

Note: Expansion respects the Roberge-Weiss symmetry, $Z(T,\mu_B) = Z(T,\mu_B + i\,2\pi T)$

Expected asymptotics

- At low T/densities QCD $\simeq$ ideal hadron resonance gas

$$\frac{p^{\mathrm{hrg}}(T,\mu_B)}{T^4} = \frac{\phi_M(T)}{T^3} + 2\,\frac{\phi_B(T)}{T^3}\cosh\left(\frac{\mu_B}{T}\right),$$

$$\phi_B(T) = \sum_{i\in B}\int dm\,\rho_i(m)\,\frac{d_i\,m^2\,T}{2\pi^2}\,K_2\left(\frac{m}{T}\right),$$

$$p_0^{hrg}(T) = \frac{\phi_M(T)}{T^3},\quad p_1^{hrg}(T) = \frac{2\,\phi_B(T)}{T^3},\quad p_k^{\mathrm{hrg}}(T) \equiv 0,\ k \geq 2$$

- At high T QCD $\simeq$ ideal gas of massless quarks and gluons

$$\frac{p^{\mathrm{SB}}(T,\mu_B)}{T^4} = \frac{8\pi^2}{45} + \sum_{f=u,d,s}\left[\frac{7\pi^2}{60} + \frac{1}{2}\left(\frac{\mu_B}{3T}\right)^2 + \frac{1}{4\pi^2}\left(\frac{\mu_B}{3T}\right)^4\right],$$

$$p_0^{\mathrm{SB}} = \frac{64\pi^2}{135},\quad p_k^{\mathrm{SB}} = \frac{(-1)^{k+1}}{k^2}\,\frac{4\,[3+4\,(\pi k)^2]}{27\,(\pi k)^2},\quad b_k^{SB} = k\,p_k^{\mathrm{SB}}.$$

Lattice data explore intermediate, transition region $130 < T < 230$ *MeV*

*In this study we assume that $\mu_S = \mu_Q = 0$

Lattice QCD results on imaginary μ_B observables

Coefficients $b_k(T)$ of ρ_B expansion are now calculated on the lattice

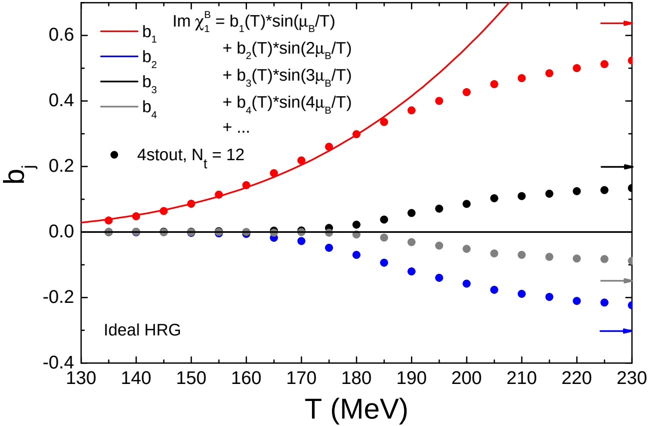

- Ideal HRG describes well $b_1(T)$ at small temperatures
- All four coefficients converge slowly to Stefan-Boltzmann limit
- What is the mechanism of appearance of non-zero b_k for $k > 1$?

V.V., A. Pásztor, Z. Fodor, S.D. Katz, H. Stoecker, 1708.02852; S. Borsányi, QM2017

Imaginary μ_B and repulsive baryonic interactions

Repulsive interactions with excluded-volume [Rischke et al., Z. Phys. C '91]

$$V \to V - bN \qquad \Rightarrow \qquad p_B(T,\mu_B) = p_B^{\rm id}(T,\mu_B - b p_B)$$

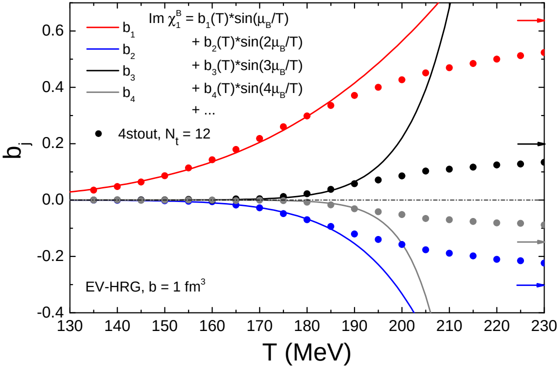

HRG with baryonic EV:

$$b_1^{\rm ev}(T) = 2\,\frac{\phi_B(T)}{T^3}$$

$$b_2^{\rm ev}(T) = -4\,[bT^3]\,\left[\frac{\phi_B(T)}{T^3}\right]^2$$

$$b_3^{\rm ev}(T) = 9\,[bT^3]^2\,\left[\frac{\phi_B(T)}{T^3}\right]^3$$

$$b_4^{\rm ev}(T) = -\frac{64}{3}\,[bT^3]^3\,\left[\frac{\phi_B(T)}{T^3}\right]^4$$

- Ideal HRG describes well $b_1(T)$ at small temperatures
- Non-zero $b_j(T)$ for $j \geq 2$ signal deviations from ideal HRG
- EV interactions between baryons ($b \simeq 1$ fm^3) reproduce lattice trend

V.V., A. Pásztor, Z. Fodor, S. Katz, H. Stoecker, 1708.02852; S. Borsányi, QM2017

Relation between leading and higher order coefficients

A particular feature of the EV model: temperature-independent ratios

$$\alpha_3 = \frac{b_1(T)}{[b_2(T)]^2} b_3(T), \qquad \alpha_4 = \frac{[b_1(T)]^2}{[b_2(T)]^3} b_4(T), \quad \ldots \quad \alpha_k = \frac{[b_1(T)]^{k-2}}{[b_2(T)]^{k-1}} b_k(T)$$

Also hold true for many other models with short-range interaction

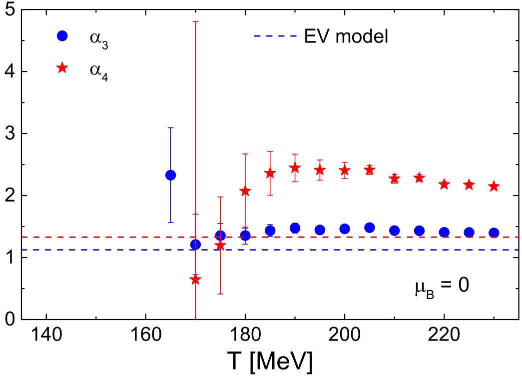

Excluded volume model:

$\alpha_3^{EV} = 1.125, \quad \alpha_4^{EV} = 1.333$

α_3 and α_4 are approximately T-independent on lattice, EV somewhat off

Relation between leading and higher order coefficients

A particular feature of the EV model: temperature-independent ratios

$$\alpha_3 = \frac{b_1(T)}{[b_2(T)]^2} b_3(T), \qquad \alpha_4 = \frac{[b_1(T)]^2}{[b_2(T)]^3} b_4(T), \quad \ldots \quad \alpha_k = \frac{[b_1(T)]^{k-2}}{[b_2(T)]^{k-1}} b_k(T)$$

Also hold true for many other models with short-range interaction

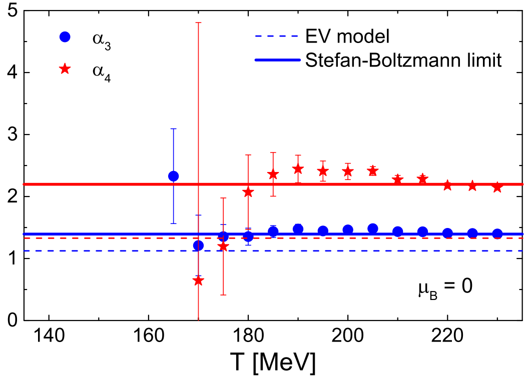

Excluded volume model:

$$\alpha_3^{EV} = 1.125, \quad \alpha_4^{EV} = 1.333$$

Stefan-Boltzmann limit of massless quarks and gluons:

$$\alpha_3^{SB} \simeq 1.394, \quad \alpha_4^{SB} \simeq 2.198$$

α_3 and α_4 are approximately T-independent on lattice, EV somewhat off

Ratios are consistent with the Stefan-Boltzmann limit of massless quarks

Cluster Expansion Model – CEM

V. Vovchenko, J. Steinheimer, O. Philipsen, H. Stoecker, 1711.01261

Cluster Expansion Model (CEM)

α_3 and α_4 are consistent with the Stefan-Boltzmann limit. Now assume the same for all higher-order coefficients

CEM formulation:

- $b_1(T)$ and $b_2(T)$ are model input
- All higher order coefficients are then predicted

$$b_k(T) = \alpha_k^{SB} \frac{[b_2(T)]^{k-1}}{[b_1(T)]^{k-2}}$$

- Observables are calculated from fugacity expansion for baryon density

$$\frac{\rho_B(T)}{T^3} = \chi_1^B(T) = \sum_{k=1}^{\infty} b_k(T) \sinh(k\, \mu_B / T)$$

- **Physical picture:** Hadron gas with residual repulsion at moderate T, weakly interacting quarks and gluons at high T

V.V., J. Steinheimer, O. Philipsen, H. Stoecker, 1711.01261

CEM: Baryon number fluctuations

Baryon number susceptibilities at $\mu_B = 0$:

$$\chi_{2n}^B(T) \equiv \left.\frac{\partial^{2n}(p/T^4)}{\partial(\mu_B/T)^{2n}}\right|_{\mu_B=0} = \sum_{k=1}^{\infty} k^{2n-1}\, b_k(T) \simeq \sum_{k=1}^{k_{\max}} k^{2n-1}\, b_k(T).$$

CEM-LQCD: $b_1(T)$ and $b_2(T)$ taken from LQCD simulations at imaginary μ_B

CEM: Baryon number fluctuations

Baryon number susceptibilities at $\mu_B = 0$:

$$\chi_{2n}^B(T) \equiv \left.\frac{\partial^{2n}(p/T^4)}{\partial(\mu_B/T)^{2n}}\right|_{\mu_B=0} = \sum_{k=1}^{\infty} k^{2n-1}\, b_k(T) \simeq \sum_{k=1}^{k_{\max}} k^{2n-1}\, b_k(T).$$

CEM-LQCD: $b_1(T)$ and $b_2(T)$ taken from LQCD simulations at imaginary μ_B

χ_2^B

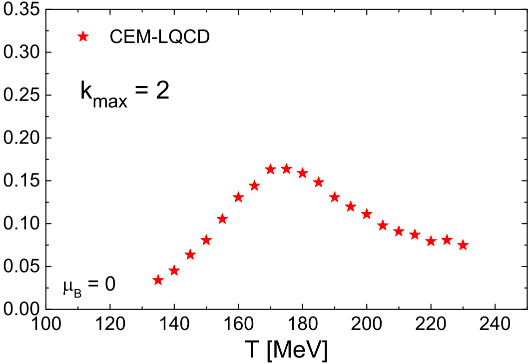

CEM: Baryon number fluctuations

Baryon number susceptibilities at $\mu_B = 0$:

$$\chi_{2n}^B(T) \equiv \left.\frac{\partial^{2n}(p/T^4)}{\partial(\mu_B/T)^{2n}}\right|_{\mu_B=0} = \sum_{k=1}^{\infty} k^{2n-1}\, b_k(T) \simeq \sum_{k=1}^{k_{\max}} k^{2n-1}\, b_k(T).$$

CEM-LQCD: $b_1(T)$ and $b_2(T)$ taken from LQCD simulations at imaginary μ_B

χ_2^B

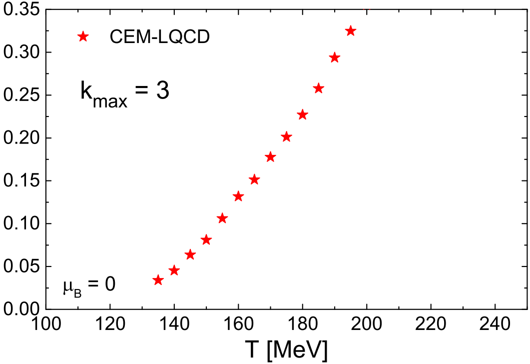

CEM: Baryon number fluctuations

Baryon number susceptibilities at $\mu_B = 0$:

$$\chi^B_{2n}(T) \equiv \left. \frac{\partial^{2n}(p/T^4)}{\partial(\mu_B/T)^{2n}} \right|_{\mu_B=0} = \sum_{k=1}^{\infty} k^{2n-1}\, b_k(T) \simeq \sum_{k=1}^{k_{\max}} k^{2n-1}\, b_k(T).$$

CEM-LQCD: $b_1(T)$ and $b_2(T)$ taken from LQCD simulations at imaginary μ_B

χ_2^B

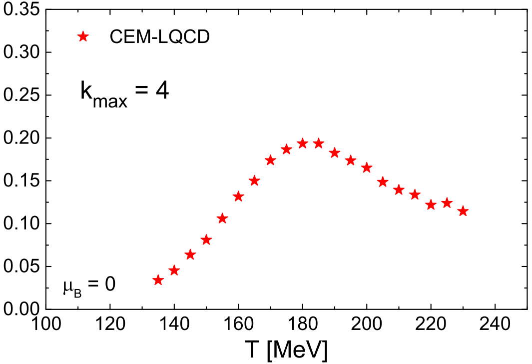

Baryon number susceptibilities at $\mu_B = 0$:

$$\chi_{2n}^B(T) \equiv \left.\frac{\partial^{2n}(p/T^4)}{\partial(\mu_B/T)^{2n}}\right|_{\mu_B=0} = \sum_{k=1}^{\infty} k^{2n-1}\, b_k(T) \simeq \sum_{k=1}^{k_{\max}} k^{2n-1}\, b_k(T).$$

CEM-LQCD: $b_1(T)$ and $b_2(T)$ taken from LQCD simulations at imaginary μ_B

χ_2^B

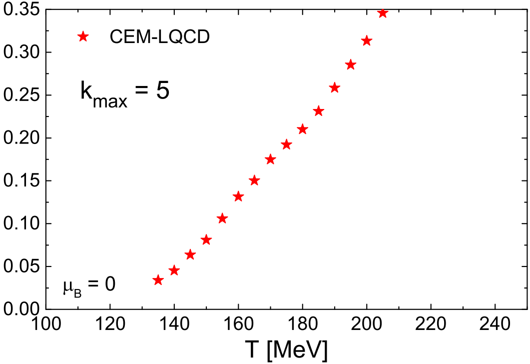

CEM: Baryon number fluctuations

Baryon number susceptibilities at $\mu_B = 0$:

$$\chi_{2n}^B(T) \equiv \left. \frac{\partial^{2n}(p/T^4)}{\partial(\mu_B/T)^{2n}} \right|_{\mu_B=0} = \sum_{k=1}^{\infty} k^{2n-1}\, b_k(T) \simeq \sum_{k=1}^{k_{\max}} k^{2n-1}\, b_k(T).$$

CEM-LQCD: $b_1(T)$ and $b_2(T)$ taken from LQCD simulations at imaginary μ_B

χ_2^B

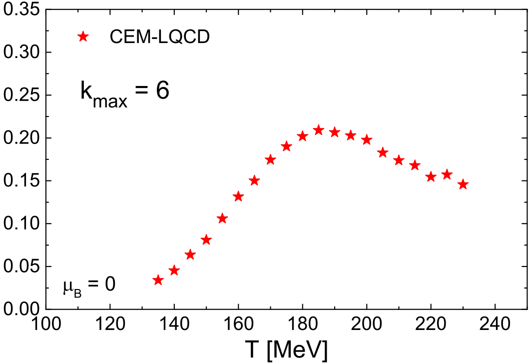

CEM: Baryon number fluctuations

Baryon number susceptibilities at $\mu_B = 0$:

$$\chi_{2n}^B(T) \equiv \left. \frac{\partial^{2n}(p/T^4)}{\partial(\mu_B/T)^{2n}} \right|_{\mu_B=0} = \sum_{k=1}^{\infty} k^{2n-1}\, b_k(T) \simeq \sum_{k=1}^{k_{\max}} k^{2n-1}\, b_k(T).$$

CEM-LQCD: $b_1(T)$ and $b_2(T)$ taken from LQCD simulations at imaginary μ_B

χ_2^B

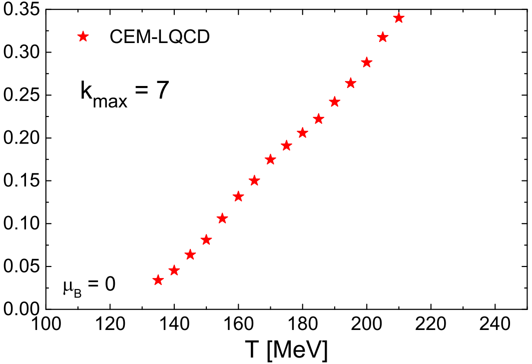

CEM: Baryon number fluctuations

Baryon number susceptibilities at $\mu_B = 0$:

$$\chi_{2n}^B(T) \equiv \left.\frac{\partial^{2n}(p/T^4)}{\partial(\mu_B/T)^{2n}}\right|_{\mu_B=0} = \sum_{k=1}^{\infty} k^{2n-1}\, b_k(T) \simeq \sum_{k=1}^{k_{\max}} k^{2n-1}\, b_k(T).$$

CEM-LQCD: $b_1(T)$ and $b_2(T)$ taken from LQCD simulations at imaginary μ_B

χ_2^B

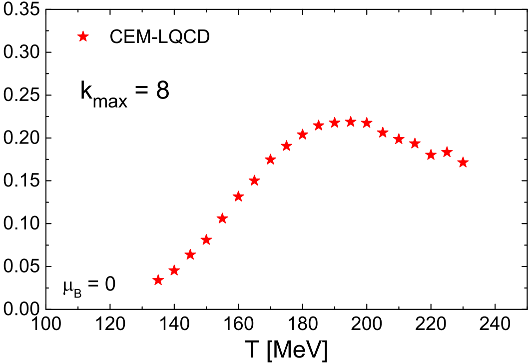

Baryon number susceptibilities at $\mu_B = 0$:

$$\chi_{2n}^B(T) \equiv \left.\frac{\partial^{2n}(p/T^4)}{\partial(\mu_B/T)^{2n}}\right|_{\mu_B=0} = \sum_{k=1}^{\infty} k^{2n-1}\, b_k(T) \simeq \sum_{k=1}^{k_{\rm max}} k^{2n-1}\, b_k(T).$$

CEM-LQCD: $b_1(T)$ and $b_2(T)$ taken from LQCD simulations at imaginary μ_B

χ_2^B

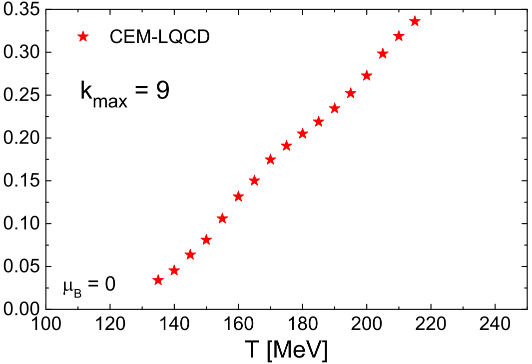

CEM: Baryon number fluctuations

Baryon number susceptibilities at $\mu_B = 0$:

$$\chi_{2n}^B(T) \equiv \left.\frac{\partial^{2n}(p/T^4)}{\partial(\mu_B/T)^{2n}}\right|_{\mu_B=0} = \sum_{k=1}^{\infty} k^{2n-1}\, b_k(T) \simeq \sum_{k=1}^{k_{\max}} k^{2n-1}\, b_k(T).$$

CEM-LQCD: $b_1(T)$ and $b_2(T)$ taken from LQCD simulations at imaginary μ_B

χ_2^B

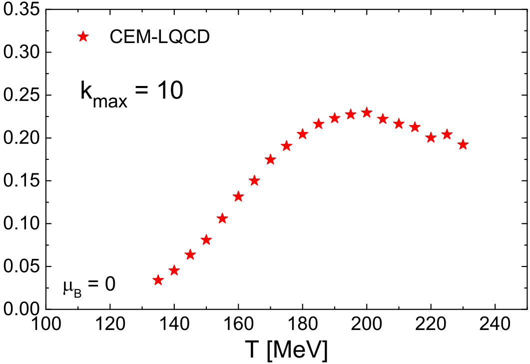

Baryon number susceptibilities at $\mu_B = 0$:

$$\chi_{2n}^B(T) \equiv \left.\frac{\partial^{2n}(p/T^4)}{\partial(\mu_B/T)^{2n}}\right|_{\mu_B=0} = \sum_{k=1}^{\infty} k^{2n-1}\, b_k(T) \simeq \sum_{k=1}^{k_{\max}} k^{2n-1}\, b_k(T).$$

CEM-LQCD: $b_1(T)$ and $b_2(T)$ taken from LQCD simulations at imaginary μ_B

χ_2^B

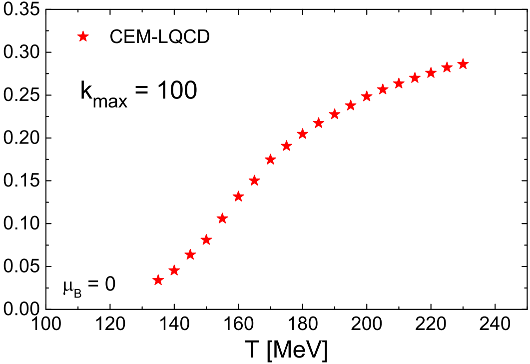

CEM: Baryon number fluctuations

Baryon number susceptibilities at $\mu_B = 0$:

$$\chi_{2n}^B(T) \equiv \left.\frac{\partial^{2n}(p/T^4)}{\partial(\mu_B/T)^{2n}}\right|_{\mu_B=0} = \sum_{k=1}^{\infty} k^{2n-1}\, b_k(T) \simeq \sum_{k=1}^{k_{\max}} k^{2n-1}\, b_k(T).$$

CEM-LQCD: $b_1(T)$ and $b_2(T)$ taken from LQCD simulations at imaginary μ_B

χ_2^B

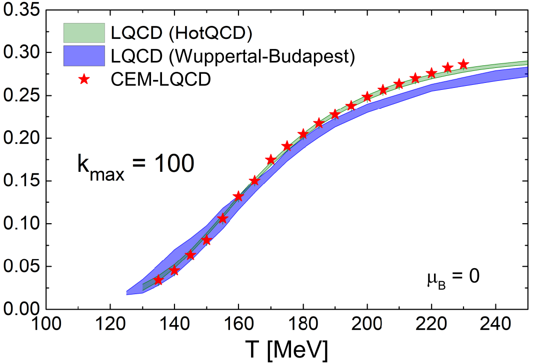

Implicit evidence for consistency between WB and HotQCD data

CEM: 4th and 6th order ratios

$$\chi_{2n}^B(T) \equiv \left.\frac{\partial^{2n}(p/T^4)}{\partial(\mu_B/T)^{2n}}\right|_{\mu_B=0} = \sum_{k=1}^{\infty} k^{2n-1}\, b_k(T).$$

χ_4^B/χ_2^B

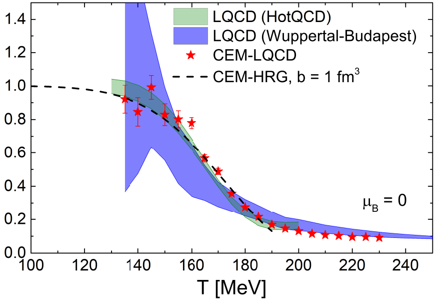

χ_6^B/χ_2^B

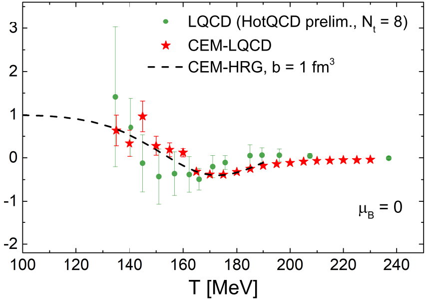

- Consistency with available LQCD data
- Interacting hadrons (CEM-HRG) up to $T \simeq 185$ MeV?

LQCD data from 1507.04627 (Wuppertal-Budapest), 1701.04325 & 1708.04897 (HotQCD)
CEM-HRG: $b_1(T)$ and $b_2(T)$ from EV-HRG model with $b = 1$ fm^3

CEM: predictions for high orders

$$\chi_{2n}^{B}(T) \equiv \left.\frac{\partial^{2n}(p/T^4)}{\partial(\mu_B/T)^{2n}}\right|_{\mu_B=0} = \sum_{k=1}^{\infty} k^{2n-1}\, b_k(T).$$

χ_8^B

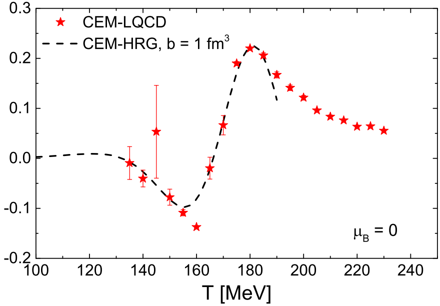

χ_{10}^B

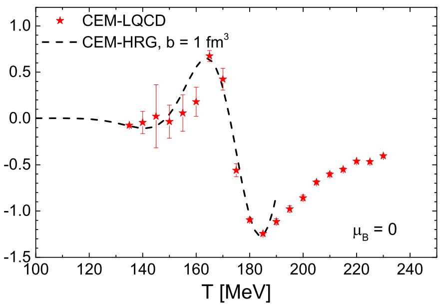

To be verified by the future lattice data

Radius of convergence

Taylor expansion of QCD pressure:

$$\frac{p(T,\mu_B)}{T^4} = \frac{p(T,0)}{T^4} + \frac{\chi_2^B(T)}{2!}(\mu_B/T)^2 + \frac{\chi_4^B(T)}{4!}(\mu_B/T)^4 + \dots$$

Radius of convergence $r_{\mu/T}$ of the expansion is the distance to the nearest singularity of p/T^4 in the *complex* μ_B/T plane at a given temperature T

If the nearest singularity is at a real μ_B/T value, this could point to the QCD critical point

Lattice QCD strategy: Estimate $r_{\mu/T}$ from few leading terms

M. D'Elia et al., 1611.08285; S. Datta et al., 1612.06673; A. Bazavov et al., 1701.04325

Ratio estimator: $$r_n = \left| \frac{(2n+2)(2n+1)\chi_{2n}^B}{\chi_{2n+2}^B} \right|^{1/2}, \qquad r_{\mu/T} = \lim_{n\to\infty} r_n$$

CEM allows to analyze r_n to very high order

Radius of convergence: Domb-Sykes plot

Domb-Sykes plot: $1/r_n^2$ vs $1/n$, linear extrapolation to $1/n = 0$ yields $r_{\mu/T}$

CEM-LQCD @ $T = 160$ MeV

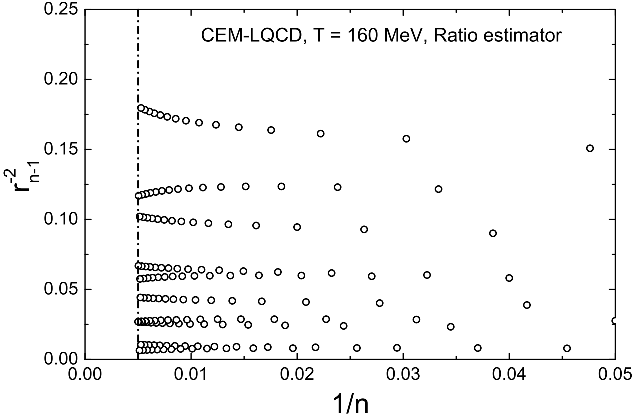

$$\lim_{n\to\infty} \left| \frac{(2n+2)(2n+1)\chi^B_{2n}}{\chi^B_{2n+2}} \right|^{1/2}$$ DOES NOT EXIST!

Radius of convergence: Structure of Taylor coefficients

Ratio estimator works when coefficients have regular asymptotic structure: they either share the same sign or they alternate in sign

Equivalently: *Limiting singularity must be at a real* $(\mu_B/T)^2$ *value*

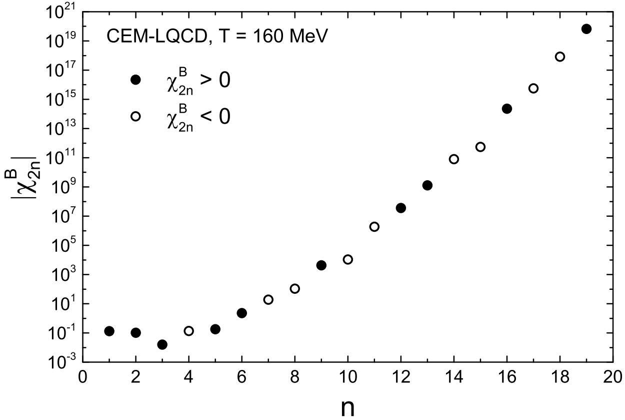

Negative coefficients appear starting from χ^B_8

Radius of convergence: Structure of Taylor coefficients

Ratio estimator works when coefficients have regular asymptotic structure: they either share the same sign or they alternate in sign

Equivalently: *Limiting singularity must be at a real* $(\mu_B/T)^2$ *value*

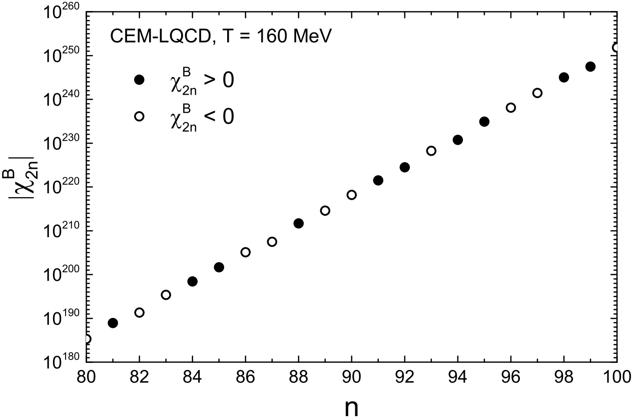

Negative coefficients appear starting from χ^B_8

They never settle into a regular pattern

This means that limiting singularity lies in the *complex* μ_B/T plane

Radius of convergence: Use ratio estimator with care!

If the limiting singularity lies in the complex μ_B/T and the ratio estimator is applied then. . .

Radius of convergence: Use ratio estimator with care!

If the limiting singularity lies in the complex μ_B/T and the ratio estimator is applied then...

Garbage in,

$$r_n = \left| \frac{(2n+2)(2n+1)\chi^B_{2n}}{\chi^B_{2n+2}} \right|^{1/2}$$

Radius of convergence: Use ratio estimator with care!

If the limiting singularity lies in the complex μ_B/T and the ratio estimator is applied then...

Garbage in,

$$r_n = \left| \frac{(2n+2)(2n+1)\chi^B_{2n}}{\chi^B_{2n+2}} \right|^{1/2}$$

Garbage out

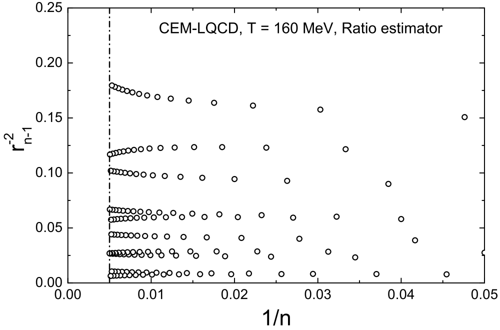

principle applies

Radius of convergence: Mercer-Roberts estimator

A more involved Mercer-Roberts estimator:

$$r_n = \left| \frac{c_{n+1}\, c_{n-1} - c_n^2}{c_{n+2}\, c_n - c_{n+1}^2} \right|^{1/4}, \qquad c_n = \frac{\chi_{2n}^B}{(2n)!}.$$

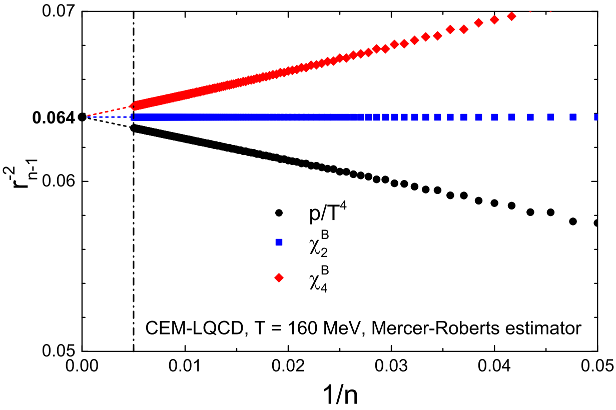

Taylor expansions for p/T^4, χ_2^B, and χ_4^B all point to the same

$\lim_{n\to\infty} r_n^{-2} \simeq 0.064 \quad \Rightarrow \quad r_{\mu/T} \simeq 3.95$ at $T = 160$ MeV

Radius of convergence: Temperature dependence

Applying the Mercer-Roberts same procedure at other temperatures

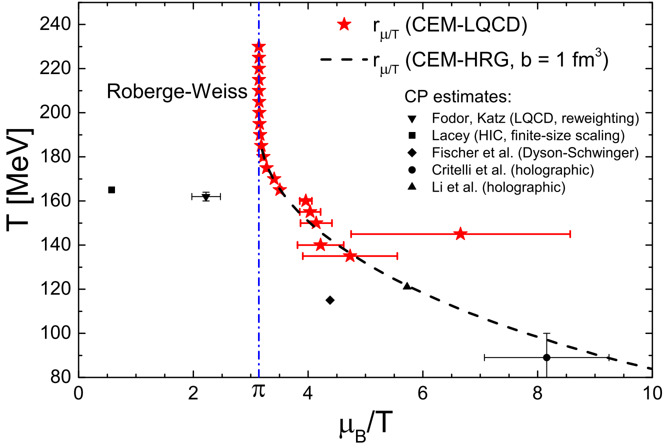

Radius of convergence of Taylor expansion sees Roberge-Weiss transition?

R-W transition expected at $T > T_{RW}$ and $\mathrm{Im}[\mu_B/T] = \pi$ [Roberge, Weiss, NPB '86]

Lattice estimate: $T_{RW} \sim 200$ MeV [C. Bonati et al., 1602.01426]

Critical point of nuclear matter and beam energy dependence of net proton number fluctuations

V. Vovchenko, L. Jiang, M. Gorenstein, H. Stoecker, 1711.07260

Critical point of nuclear matter

While the existence and location of the QCD critical point is unclear, the QCD phase diagram

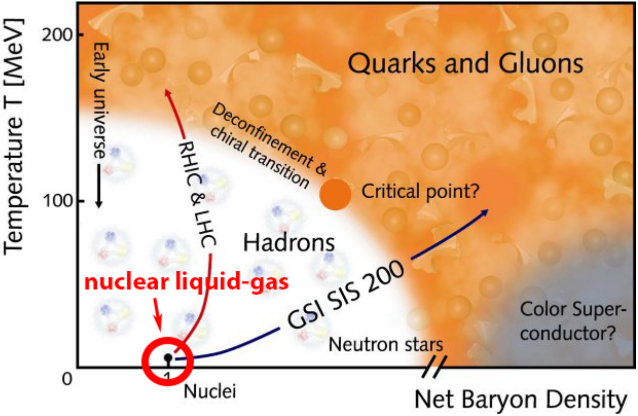

is known to contain the critical point of nuclear matter at $T_c \sim 15$ MeV and *real* $(c\mu_B/T)_c \sim 40$

How does it influence the fluctuation observables in heavy-ion collisions?

QvdW-HRG model [**V.V.**, M.I. Gorenstein, H. Stoecker, PRL 118, 182301 (2017)]

HRG with attractive and repulsive van der Waals interactions between baryons

vdW parameters $a = 329$ MeV fm^3 and $b = 3.42$ fm^3 tuned to nuclear ground state properties

Critical point of nuclear matter at $T_c \simeq 19.7$ MeV, $\mu_c \simeq 908$ MeV

Hadronic model – no QGP

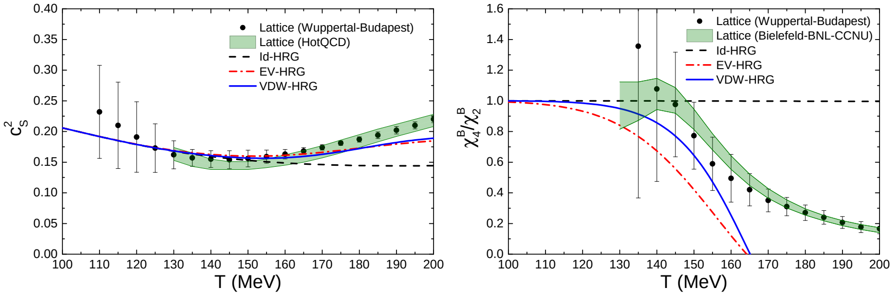

Strong effects even at $\mu_B = 0$!

What about intermediate collision energies?

QvdW-HRG model: fluctuations in T-μ_B plane

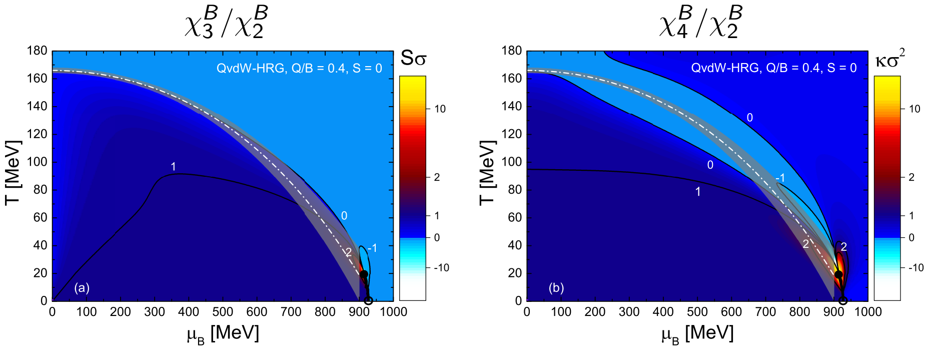

Chemical freeze-out curve from *Cleymans et al., Phys. Rev. C 73, 034905 (2006)*

Critical point of nuclear matter shines brightly in fluctuation observables, across the whole region of phase diagram probed by heavy-ion collisions

QvdW-HRG model: collision energy dependence

Calculating fluctuations along the “freeze-out” curve

Acceptance effects (protons instead of baryons, momentum cut) modeled *schematically*, by applying the *binomial filter* [A. Bzdak, V. Koch, PRC ’12]

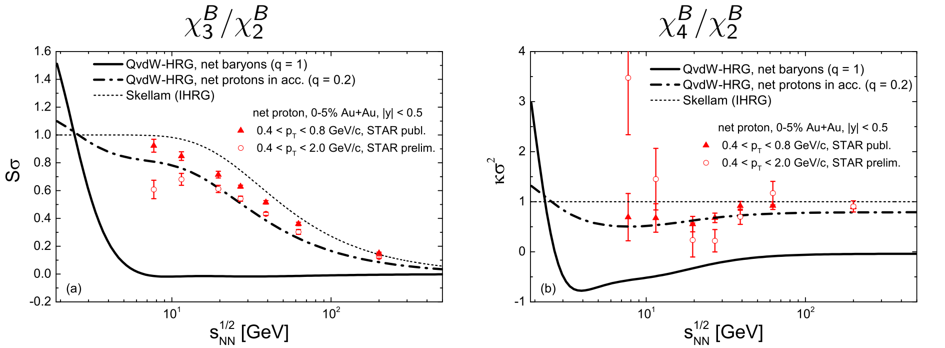

Effects of nuclear liquid-gas criticality:

- Non-monotonic collision energy dependence
- Net proton quite different from net baryon, even if global charge conservation effects could be neglected/corrected for

Scenarios for collision energy dependence

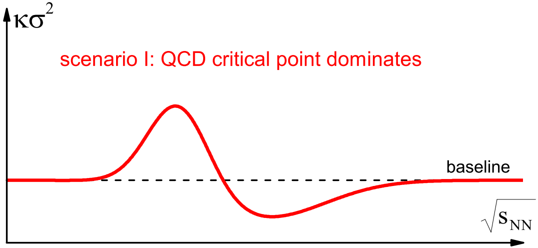

M. Stephanov, JPG "11

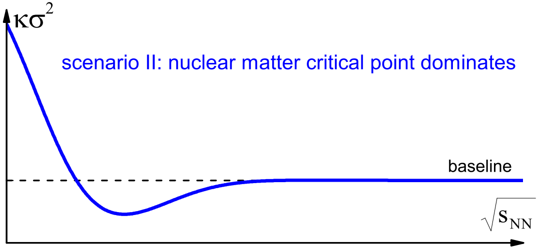

V.V., *L. Jiang, M. Gorenstein, H. Stoecker, 1711.07260*

Can the scenarios be distinguished? Need data at lower energies...

Opportunities for HADES, CBM, NA61/SHINE, STAR!

Summary

- LQCD data at imaginary μ_B suggests presence of repulsive baryonic interactions with "eigenvolume" $b \simeq 1$ fm^3 in the crossover region

- Cluster Expansion Model describes all available lattice data on net baryon susceptibilities. Radius of convergence at $T > 135$ MeV sees Roberge-Weiss like transition in the complex μ_B/T plane

- Nuclear liquid-gas criticality causes non-monotonic energy dependence of skewness and kurtosis

- Net proton fluctuations $\neq$ Net baryon fluctuations, for more reasons than just baryon number conservation

Summary

- LQCD data at imaginary μ_B suggests presence of repulsive baryonic interactions with "eigenvolume" $b \simeq 1$ fm^3 in the crossover region
- Cluster Expansion Model describes all available lattice data on net baryon susceptibilities. Radius of convergence at $T > 135$ MeV sees Roberge-Weiss like transition in the complex μ_B/T plane
- Nuclear liquid-gas criticality causes non-monotonic energy dependence of skewness and kurtosis
- Net proton fluctuations $\neq$ Net baryon fluctuations, for more reasons than just baryon number conservation

Thanks for your attention!

Backup slides

Baryonic excluded volume

Baryon-baryon interactions seem to exhibit a repulsive core – excluded volume

EV model: a simple approach for repulsive interactions [Rischke et al., Z. Phys. C '91]

$$V \to V - bN \qquad \Rightarrow \qquad p(T,\mu) = p^{\rm id}(T, \mu - bp)$$

EV-HRG model

- Identical EV interactions for all baryon-baryon and antibaryon-antibaryon pairs
- Baryon-antibaryon, meson-meson, meson-baryon EV terms neglected
- A single parameter b characterizing interactions

Three independent subsystems: mesons + baryons + antibaryons

$$p(T,\boldsymbol{\mu}) = p_M(T,\boldsymbol{\mu}) + p_B(T,\boldsymbol{\mu}) + p_{\bar{B}}(T,\boldsymbol{\mu}),$$

$$p_M(T,\boldsymbol{\mu}) = \sum_{j \in M} p_j^{\rm id}(T,\mu_j) \quad \text{and} \quad p_B(T,\boldsymbol{\mu}) = \sum_{j \in B} p_j^{\rm id}(T,\mu_j - b\, p_B)$$

“Excluded volume” parameter from imaginary μ_B data

“Excluded volume” parameter of baryon-baryon interactions can be estimated from lattice

$$b(T) = -\frac{b_2(T)}{[b_1(T)]^2\, T^3}$$

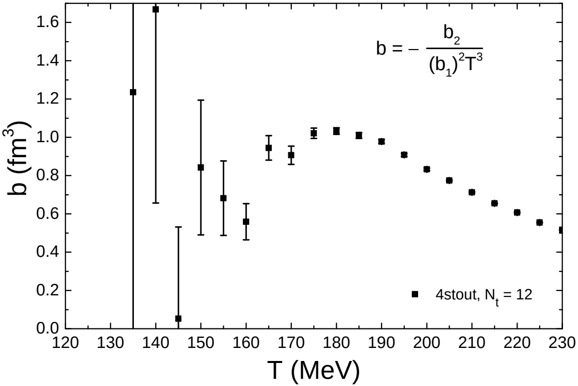

$b(T)$ mostly consistent with 1 fm^3 at $T < 190$ MeV

V.V., A. Pásztor, Z. Fodor, S.D. Katz, H. Stoecker, 1708.02852

Radius of convergence: Cross-check with Padé approximants

Padé approximant for χ_2^B:

$$\chi_2^B(T,\mu_B/T) \approx \frac{\sum_{j=0}^{m} a_j\,(\mu_B/T)^j}{1+\sum_{k=1}^{n} b_k\,(\mu_B/T)^k}$$

a_j and b_k constructed from χ_{2n}^B to match Taylor expansion

Poles of Padé approximants often point to true singularities of the function

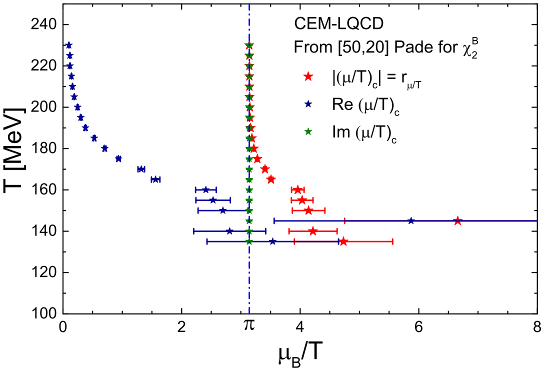

$\mathrm{Im}[\mu_B/T]_c = \pi$, while $\mathrm{Re}[\mu_B/T]_c$ decreases towards zero with

Going beyond the radius of convergence

Padé approximants allow to go beyond the radius for convergence

Example: χ_4^B/χ_2^B at finite μ_B/T

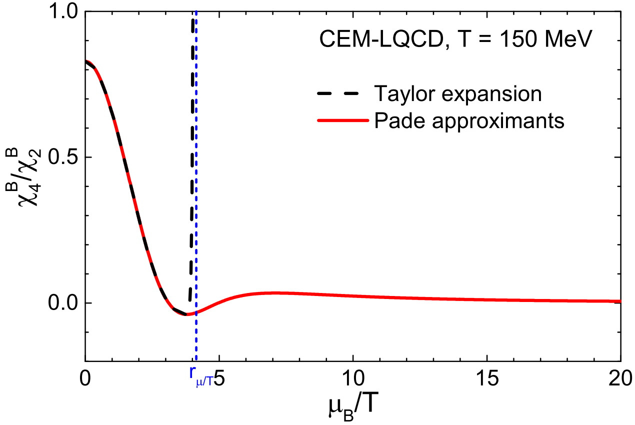

Outlook: Full QCD equation of state at finite baryon density

Full QCD equation of state at finite baryon density can be obtained from fugacity expansion

$$\frac{p(T,\mu_B)}{T^4} = \frac{p(T,0)}{T^4} + \sum_{k=1}^{\infty} \frac{b_k(T)}{k} \left[\cosh(k\,\mu_B/T) - 1\right],$$

or from Taylor expansion

$$\frac{p(T,\mu_B)}{T^4} = \frac{p(T,0)}{T^4} + \sum_{k=1}^{\infty} \frac{\chi_{2k}^{B}(T)}{(2k)!} \left(\mu_B/T\right)^{2k},$$

where $p(T,0)/T^4$ is already available from lattice QCD, and where $b_k(T)$ or $\chi_{2k}^{B}(T)$ can be computed using CEM to arbitrary order.

Various techniques can be employed to circumvent limitations due to a finite radius of convergence.